NIH Public Access
Author Manuscript
Sci Transl Med. Author manuscript; available in PMC 2011 September 2.

Published in final edited form as:
Sci Transl Med. 2011 March 2; 3(72): 72ra18. doi:10.1126/scitranslmed.3001777.

Antisense Oligonucleotides Delivered to the Mouse CNS Ameliorate Symptoms of Severe Spinal Muscular Atrophy

Marco A. Passini[1,*], **Jie Bu**[1], **Amy M. Richards**[1], **Cathrine Kinnecom**[1], **S. Pablo Sardi**[1], **Lisa M. Stanek**[1], **Yimin Hua**[2], **Frank Rigo**[3], **John Matson**[3], **Gene Hung**[3], **Edward M. Kaye**[1,4], **Lamya S. Shihabuddin**[1], **Adrian R. Krainer**[2], **C. Frank Bennett**[3], and **Seng H. Cheng**[1]

[1]Genzyme Corporation, 49 New York Avenue, Framingham, MA 01701, USA.

[2]Cold Spring Harbor Laboratory, 1 Bungtown Road, Cold Spring Harbor, NY 11724, USA.

[3]Isis Pharmaceuticals, 1896 Rutherford Road, Carlsbad, CA 92008, USA.

[4]Department of Neurology, Harvard Medical School, 300 Longwood Avenue, Boston, MA 02114, USA.

Abstract

Spinal muscular atrophy (SMA) is an autosomal recessive neuromuscular disorder caused by mutations in the SMN1 gene that result in a deficiency of SMN protein. One approach to treat SMA is to use antisense oligonucleotides (ASOs) to redirect the splicing of a paralogous gene, *SMN2*, to boost production of functional SMN. Injection of a 2′-*O*-2-methoxyethyl–modified ASO (ASO-10-27) into the cerebral lateral ventricles of mice with a severe form of SMA resulted in splice-mediated increases in SMN protein and in the number of motor neurons in the spinal cord, which led to improvements in muscle physiology, motor function and survival. Intrathecal infusion of ASO-10-27 into cynomolgus monkeys delivered putative therapeutic levels of the oligonucleotide to all regions of the spinal cord. These data demonstrate that central nervous system–directed ASO therapy is efficacious and that intrathecal infusion may represent a practical route for delivering this therapeutic in the clinic.

Copyright 2011 by the American Association for the Advancement of Science; all rights reserved.

[*]To whom correspondence should be addressed. marco.passini@genzyme.com.

Author contributions: M.A.P. designed and executed the experiments, analyzed the data, and wrote the manuscript; J.B. (Figs. 1, 3, and 4), A.M.R. (Figs. 2 and 5), C.K. (Fig. 2), S.P.S. (Fig. 2), L.M.S. (Fig. 5), Y.H. (Fig. 2), F.R. (Figs. 2 and 6), and G.H. (Figs. 2 and 6) assisted with the experiments and analysis; J.M. generated the oligonucleotides; E.M.K. and L.S.S. assisted with analysis; A.R.K., C.F.B., and S.H.C. assisted with analysis and writing of the manuscript.

SUPPLEMENTARY MATERIAL
www.sciencetranslationalmedicine.org/cgi/content/full/3/72/72ra18/DC1 Fig. S1. Distribution of ASO-10-27 in the brain after intracerebroventricular administration. Fig. S2. Splicing of SMN2 in the liver at 16 days. Fig. S3. SMN Western blots of the thoracic region at 3, 16, and 30 days. Fig. S4. Behavioral performances and weight changes in treated wild-type mice. Fig. S5. H&E staining of the cynomolgus brain and spinal cord.

Competing interests: M.A.P., J.B., A.M.R., C.K., S.P.S., L.M.S., E.M.K., L.S.S., and S.H.C. are paid employees of Genzyme Corporation; F.R., J.M., G.H., and C.F.B. are paid employees of Isis Pharmaceuticals; C.F.B. is an executive officer of Isis Pharmaceuticals; A.R.K. is a paid consultant for Isis Pharmaceuticals. Isis Pharmaceuticals has filed joint patents on the subject matter with Cold Spring Harbor Laboratory (WO 2007/002390), and with Cold Spring Harbor Laboratory and Genzyme Corporation (WO 2010/148249). Isis Pharmaceuticals holds the patent (US 5,914,396) on the oligonucleotide chemistry used in this study. Isis Pharmaceuticals has licensed IP (US 7,838,657) from the University of Massachusetts that covers the sequence of the intronic splicing silencer that is targeted by ASO-10-27.

Citation: M. A. Passini, J. Bu, A. M. Richards, C. Kinnecom, S. P. Sardi, L. M. Stanek, Y. Hua, F. Rigo, J. Matson, G. Hung, E. M. Kaye, L. S. Shihabuddin, A. R. Krainer, C. F. Bennett, S. H. Cheng, Antisense oligonucleotides delivered to the mouse CNS ameliorate symptoms of severe spinal muscular atrophy. *Sci. Transl. Med.* **3**, 72ra18 (2011).

NIH-PA Author Manuscript
NIH-PA Author Manuscript
NIH-PA Author Manuscript

NIH-PA Author Manuscript

NIH-PA Author Manuscript

NIH-PA Author Manuscript

INTRODUCTION

Spinal muscular atrophy (SMA) is a childhood neuromuscular disease caused by mutations in the *SMN1* locus and a substantial decrease in SMN protein (*1*). The deficiency in SMN protein leads to the progressive loss of motor neurons in the spinal cord and resultant skeletal muscle atrophy (*2*). Paralysis, brainstem (bulbar) defects, and respiratory defects are the primary manifestations of this disease and ultimately lead to a shortened life span and death of patients (*3*). The severity of SMA is dictated in part by the copy number of the related duplicated gene *SMN2*, which has a critical C-to-T transition in an exonic splicing enhancer site of exon *7* (*4–7*). The base substitution at this position is translationally silent, but it impairs the ability of the spliceosome to recognize exon 7; consequently, this exon is excluded in most mature mRNA transcripts (*5*, *6*). Aberrant mRNA transcripts lacking exon *7* encode a truncated and unstable protein (SMNΔ7). However, despite the base substitution in the exonic splicing enhancer, the spliceosome is still capable of generating a small percentage of *SMN2* mRNAs that incorporate exon *7* (*8*). Thus, a small amount of SMN is generated by virtue of alternative splicing of *SMN2*, which explains the clinical observation that more copies of *SMN2* are associated with less severe forms of the disease. Indeed, the effect of *SMN2* copy number is clearly evident in clinical cases, showing that humans lacking both *SMN1* alleles but with five copies of *SMN2* do not develop SMA (*9*).

Several putative therapeutic strategies have been proposed for the management of SMA. These include *SMN1* gene replacement using viral vectors carrying the wild-type human *SMN1* complementary DNA (*cDNA*) (*10–13*) or by stem cell transplantation (*14*, *15*). In particular, mice with severe SMA treated with adeno-associated viral (AAV) vectors encoding the human SMN protein resulted in a log-fold increase in median survival in an animal model that historically has been refractory to therapy (*11*, *12*). Recent reports in the adult cat (*16*) and newborn monkey (*11*) showed promising results that a subset of spinal cord motor neurons can become transduced by systemic injections of AAV, and additional studies are under way to improve delivery of viral vectors across the blood-brain barrier and cerebrospinal-pial barrier in large-animal models.

Alternatives to gene replacement are small-molecule drugs that modulate endogenous *SMN2*, and these have also been effective in increasing SMN levels in vivo. For example, histone deacetylase inhibitors and quinazoline compounds increase *SMN2* mRNA levels and improve a variety of phenotypes in mouse models of SMA (*17–21*). Furthermore, aminoglycoside compounds promote stop-codon read-through of SMNΔ7 to generate a longer, more functional version of the truncated protein (*22*). Another attractive strategy is to alter the splicing pattern of *SMN2* so that a larger percentage of the translated protein is SMN. This has been realized with several classes of small-molecule drugs that increase SMN levels by increasing the processes that favor exon *7* inclusion (*23*, *24*). Although small-molecule drugs have been beneficial in cell lines derived from patients with SMA and in mouse models, those that have been tested in patients with SMA have shown little success, underscoring the need to develop new therapies to treat this neuromuscular disease (*25–27*).

An alternative approach to alter the splicing pattern of *SMN2* is to use antisense oligonucleotides (ASOs). ASOs are designed to base pair to specific nucleotide sequences, and thus, they potentially offer a lower risk for off-target effects than do small-molecule drugs. Systematic tiling of *SMN2* pre-mRNAs derived from intron 6, exon *7*, and intron *7* has identified ASOs that promote exon *7* inclusion and a corresponding increase in SMN protein (*28*, *29*). In particular, in vitro assays showed that blocking the intronic splicing silencer of the 5′ region of *SMN2* intron *7* (ISS-N1) with ASOs provided the most efficient increase in exon *7* inclusion (*30*, *31*); no off-target splicing of mini-genes was detected (*30*).

NIH-PA Author Manuscript

NIH-PA Author Manuscript

NIH-PA Author Manuscript

The hybridization of ASOs to the ISS-N1 region displaces trans-acting negative repressors and/or unwinds a cis-acting RNA stem-loop that interferes with the binding of U1 small nuclear RNA at the 5′ splice site of exon *7* (*29*, *32*).

Testing of such ASOs with 2′-*O*-methyl (2′-OMe) chemistry showed that multiple injections over time were required to affect SMN levels in vivo (*33*). To improve the efficacy of the ASO for more relevant clinical application, we incorporated a uniform 2′-*O*-2-methoxyethyl (MOE) chemistry into the ribose sugars, in addition to phosphorothioate substitution of the backbone. The uniform base modification does not support the degradation of the target RNA by ribonuclease (RNase) H–dependent or RNA interference (RNAi) pathways (*34*). Here, we tested whether a single administration of MOE ASO-10-27, which targets the ISS-N1 region of human *SMN2*, is efficacious in a severe mouse model of SMA. Our data show that central nervous system (CNS) delivery of ASO-10-27 improves muscle physiology, motor function, and survival in mice with a severe form of SMA. Furthermore, we show that presumptively therapeutic levels of ASO-10-27 could be delivered to the spinal cord of a nonhuman primate (NHP) using a simple intrathecal infusion strategy. The efficacy of ASO-10-27 after delivery to the CNS supports further development of splice-switching antisense technology for SMA.

RESULTS

Spinal cord delivery of oligonucleotide by injection of mouse cerebral lateral ventricles

We determined the biodistribution pattern of the ASO-10-27 oligo-nucleotide after intracerebroventricular injection of newborn mice. Heterozygous pups ($Smn^{+/-}$, $hSMN2^{+/+}$, $SMN\Delta7^{+/+}$) ($n = 4$) were injected with 8 μg of ASO-10-27 at postnatal day 0 (P0) and again at day 5, and then killed at day 14. This dosing strategy was selected to maximize the probability of visualizing the ASO on tissue sections. ASO-10-27 was abundant in the caudal regions of the brain and in the dorsal and ventral horns of the spinal cord, which is consistent with the directional flow of cerebrospinal fluid from the cerebral lateral ventricles (fig. S1). Colocalization studies using choline acetyltransferase (ChAT) staining showed that the vast majority (94 to 96%) of the motor neurons in the cervical, thoracic, and lumbar regions also stained positively for ASO-10-27 (Fig. 1).

ASO-10-27 increased exon 7 inclusion and SMN levels in the spinal cord

To determine the effect of ASO-10-27 on *SMN2* splicing and SMN protein levels, we injected a single 4-μg dose of either ASO-10-27 or an ASO-mismatched oligonucleotide control into the cerebral lateral ventricles of mice with severe SMA ($Smn^{-/-}$, $hSMN2^{+/+}$, $SMN\Delta7^{+/+}$) on the day of birth (P0). Drug- and control-treated mice with severe SMA were killed 16 days after birth, which corresponds to the typical end stage of disease in untreated mice ($n = 5$ per group). A four- to sixfold increase in full-length *SMN2*-derived mRNA transcripts (containing exon *7*) was observed in all regions of the spinal cord of ASO-10-27–treated SMA mice ($P < 0.001$) (Fig. 2A). In contrast, the levels of full-length *SMN2*-derived mRNA in the ASO-mismatch group remained the same as those in untreated SMA mice. This demonstrated that the change in alternative splicing after ASO-10-27 treatment was not due to a nonspecific, class effect of the ASOs. Concomitant with the increase in full-length *SMN2*-derived mRNA, there were higher levels of SMN throughout the spinal cord compared with control mice ($P < 0.001$) (Fig. 2B). Analysis of the liver of ASO-10-27–treated mice at 16 days showed no significant changes in *SMN2* splicing, suggesting that there was not an appreciable amount of the ASO in systemic circulation after intracerebroventricular delivery (fig. S2).

NIH-PA Author Manuscript

NIH-PA Author Manuscript

NIH-PA Author Manuscript

Pharmacokinetics and pharmacodynamics of ASO-10-27 in mice with severe SMA

The pharmacokinetics of ASO-10-27 in SMA mice injected at P0 was followed over a period of 30 days ($n = 5$ per group). Tissue concentrations of ASO-10-27, as measured in the cervical region, were highest (8 to 10 μg of ASO per gram of tissue) at 3 days ($P < 0.001$) (Fig. 2C). These levels declined to ~2 μg of ASO/g tissue at 16 days and to ~1.5 μg of ASO/g tissue at 30 days (Fig. 2C). Measurement of the levels of full-length *SMN2*-derived mRNA in the lumbar region showed a three- and sixfold increase with ASO-10-27 treatment at 3 and 16 days, respectively (Fig. 2C). However, these elevated levels of exon *7* inclusion were not sustained, returning to pretreatment levels on day 30 (Fig. 2C). This pharmacodynamic profile of the *SMN2*-derived full-length mRNA was recapitulated for the SMN protein. Western blot analysis of the thoracic region indicated that levels of SMN protein were ~50% of wild-type levels on day 3, increasing to 100% of wild-type levels on day 16, before declining to pretreatment levels on day 30 (Fig. 2C; see fig. S3 for the Western blots). Hence, ASO-10-27 has a tissue half-life of less than 2 weeks and a pharmacodynamic effect that does not extend beyond 30 days after a single bolus injection into the CNS of neonatal mice.

ASO-10-27 ameliorates the decline in motor neuron cell counts in the spinal cord

To determine the efficacy of ASO-10-27 to ameliorate cellular phenotypes, we injected SMA mice at P0 with 4 μg of ASO-10-27 or ASO-mismatched oligonucleotide and analyzed for motor neuron cell counts ($n = 5$ per group) and muscle physiology ($n = 5$ per group). The number of motor neurons in the spinal cord of untreated SMA mice was significantly lower than in wild-type mice at 16 days (Fig. 2D). The number of motor neurons in the spinal cord of SMA mice treated with ASO-mismatch was not different from those in untreated SMA controls (Fig. 2D). In contrast, mice treated with ASO-10-27 showed a significantly greater number of ChAT immunopositive cells in the cervical and thoracic regions ($P < 0.001$) (Fig. 2D). Despite successful delivery of ASO-10-27 to the lumbar region and, consequently, measurable increases in lumbar SMN levels, there was no significant improvement in the number of motor neurons in this region (Fig. 2D). However, one of the ASO-10-27–treated SMA mice did not show an increase in motor neuron cell counts in the lumbar region (for unknown reasons), thus negating the ASO-10-27–treated cohort from achieving a significant *P* value compared to the ASO-mismatch control group.

Improved muscle physiology in ASO-10-27–treated SMA mice

The size of the myofibers and the architecture of the neuromuscular junction in the quadriceps and intercostal muscles were analyzed at 16 days. These muscle groups were selected because they are severely affected in SMA and are responsible for the paralysis and respiratory defects (*2*, *3*). The cross-sectional areas of myofibers from SMA mice treated with ASO-10-27 were two- to threefold larger than ASO-mismatch–treated or untreated controls ($P < 0.001$) (Fig. 3). In addition to the increase in myofiber size, the architecture of the neuromuscular junction of SMA mice was also improved with ASO-10-27 (Fig. 4). About 75 to 80% of the neuromuscular junctions of untreated SMA mice and those administered the ASO-mismatch contained the hallmark collapse structure at the motor end plate. In contrast, the neuromuscular junctions of the quadriceps and intercostal muscles of ASO-10-27–treated SMA mice showed a significantly lower number of this abnormal phenotype at 16 days ($P < 0.001$). Furthermore, all of the neuromuscular junctions from the ASO-10-27–treated SMA mice at 30 to 40 days were innervated, with >95% exhibiting a normal architecture, indicating that correction of the neuromuscular junction was maintained over this time period (Fig. 4E).

NIH-PA Author Manuscript

NIH-PA Author Manuscript

NIH-PA Author Manuscript

ASO-10-27 improved motor function in SMA mice

We determined the functional efficacy of CNS administration of ASO-10-27 (n = 8 per group). SMA mice treated with ASO-10-27 at birth were significantly heavier than their untreated littermates on day 16, but remained smaller than age-matched wild-type controls ($P < 0.001$) (Fig. 5, A and B). Measurement of the righting reflex on day 8 in ASO-10-27–treated SMA mice showed a latency that was intermediate between untreated SMA and wild-type controls ($P < 0.001$) (Fig. 5C). However, by day 16, their performance was similar to that of wild-type mice, suggesting that treatment had improved muscle strength and coordination ($P < 0.001$) (Fig. 5D). These improvements in ASO-10-27–treated SMA mice were further substantiated by their performances on grip strength and hindlimb splay tests. In both tests, mice administered ASO-10-27 exhibited activities that were less than those of wild-type mice, but were nevertheless significantly higher than those of untreated SMA mice ($P < 0.001$) (Fig. 5, E and F). Hence, the noted improvements in myofiber size and neuromuscular junction architecture translated into functional improvements in muscle strength and coordination. Finally, treatment of wild-type mice with ASO-10-27 did not affect their performance on functional tests (fig. S4A).

ASO-10-27 enhanced mouse survival in a dose-dependent manner

To assess whether treatment with ASO-10-27 provided a survival benefit, we injected SMA mice at P0 with varying doses of the ASO ranging from 0.5 to 8 μg. Intracerebroventricular injections of 16 μg or higher resulted in a significant death rate within 24 hours of administration, indicating that an 8 μg intracerebroventricular bolus injection was the maximum tolerated dose in P0 mice. The median life spans of ASO-10-27–treated SMA mice were 23 (8 μg, n = 20), 25 (4 μg, n = 29), 23 (2 μg, n = 12), 20 (1 μg, n = 13), and 17 (0.5 μg, n = 13) days, compared to 16 days for both the ASO-mismatch–treated (4.0 μg, n = 19) and untreated (n = 30) SMA mice (Fig. 5G). Furthermore, a dose-dependent increase in weight gain was observed between P7 and P14 in treated SMA mice (Fig. 5H). Wild-type mice that received similar doses did not gain more weight compared to age-matched untreated wild-type controls (fig. S4B). This observation indicates that the positive effect on body weight in the ASO-10-27–treated SMA mice was due to efficacy and not to a non-specific drug side effect.

None of the ASO-mismatch–treated or untreated SMA mice survived to the weaning age of 21 days. In contrast, 50, 55, 50, 31, and 8% of SMA mice treated with 8, 4, 2, 1, and 0.5 μg were alive at 21 days, respectively. All of the ASO-10-27–treated SMA mice regardless of dose were ambulating and well groomed, which persisted in animals that lived beyond weaning. However, most of the weaned SMA mice were eventually found dead in their cage, indicating an acute sudden death. In some instances, weaned SMA mice developed breathing difficulties that included a decreased rate of respiration and shallow breathing. Hindlimb necrosis was observed in the treated SMA mice that lived beyond 40 days, but the necrosis did not progress to a phenotype requiring their euthanasia. The pharmacokinetic and pharmacodynamic data suggest that the ideal time to readminister ASO-10-27 would be about 10 to 14 days after treatment, when the tissue concentrations of the drug approached levels deemed to be pharmacologically inactive. However, we encountered technical and logistical difficulties in performing surgery on mice of this age, and thus were unable to address the impact of repeat dosing on median survival.

Intrathecal infusion delivered therapeutic levels of ASO-10-27 to the spinal cord of NHPs

The feasibility and practicality of delivering ASO-10-27 to the spinal cord of adult cynomolgus monkeys by intrathecal or intracerebroventricular infusion were examined. Both routes of administration are used clinically to deliver therapeutic agents. A dose of 3 mg of ASO-10-27 was infused into the intrathecal space over 1, 3, 7, or 14 days (n = 5 per

NIH-PA Author Manuscript

NIH-PA Author Manuscript

NIH-PA Author Manuscript

group) or into the right cerebral lateral ventricle over 14 days (n = 5). Each monkey was killed 5 days after completion of the infusion. There were no deaths or clinical adverse effects observed during the in-life portion of the experiment, indicating that the monkeys tolerated the infusions. Irrespective of the infusion period, monkeys treated by intrathecal infusion exhibited tissue concentrations of ASO (>8 μg/g) in the cervical, thoracic, and lumbar regions (Fig. 6A). The lumbar and thoracic regions showed the highest levels of ASO-10-27, which may have been a consequence of the placement of the catheter between the upper lumbar and lower thoracic regions of the spinal cord. The highest tissue concentrations of the ASO in the thoracic and lumbar regions were achieved when the 3-mg dose was infused over a period of 1 or 3 days (~20 to 30 μg ASO per gram tissue). Animals administered the same dose of ASO via the cerebral lateral ventricle over 14 days showed delivery of putatively therapeutic levels of ASO-10-27 (8 μg/g tissue) only in the thoracic region (Fig. 6A).

Histological analysis from monkeys treated by intrathecal infusion showed robust immunostaining for ASO-10-27 in all regions of the spinal cord (Fig. 6B). A punctate intracellular signal was observed in both large and small cell bodies, consistent with neuronal and glial cell targeting. A similar pattern of staining but with a weaker signal was also observed in the group treated by intracerebroventricular infusion. As expected, no ASO signal was detected in saline-treated controls (n = 4) (Fig. 6B). Histological examination of brain and spinal cord tissue sections stained with hematoxylin and eosin (H&E) did not reveal overt pathology attributable to the drug, further demonstrating that ASO-10-27 was well tolerated (fig. S6). However, a formal toxicology study that extends over a longer investigational period will need to be performed to understand the safety profile of ASO-10-27. The pharmacological effect of the ASO was not measured because NHPs lack the *SMN2* gene (*35*).

DISCUSSION

SMN2 evolved from the duplication and mutation of the ancestral telomeric *SMN* gene, and it is found in all extant human populations (*35*). Given that *SMN2* is capable of making a small amount of SMN protein by alternative splicing, *SMN2* serves as a viable target for therapeutic intervention in all patients with SMA. Empirical testing of a large number of MOE oligonucleotides harboring complementary sequences to *SMN2* identified an ASO (ASO-10-27) that exhibited the appropriate splicing activity in vitro, and in a transgenic mouse model without appreciable SMA phenotypes (*29*, *36*). Thus, the current report is a critical proof-of-concept study to determine whether splice-switching antisense technology can ameliorate the hallmark molecular, cellular, and functional phenotypes of a mouse model that recapitulates severe SMA disease. We show that a single administration of ASO-10-27 into the cerebral lateral ventricles of mice with severe SMA was sufficient to increase SMN protein levels by altering the *SMN2* splicing pattern, which correlated with increases in the number of motor neurons and improvements in behavior and survival. CNS-directed therapy improved muscle physiology by increasing the size of myofibers and improving the structure of the neuromuscular junction in affected skeletal muscles. The correction of muscle pathology by targeting motor neurons through intrathecal delivery of therapeutic oligonucleotides is a significant finding because it allows for a single route of administration (that is, intrathecal) to treat the disease.

A previous study that used an ASO against the ISS-N1 region of *SMN2* with a different chemistry (2′-OMe) required injections on days 1, 3, 5, 7, and 10 to affect SMN protein levels in the same severe SMA mouse model (*33*). Furthermore, the molecular mechanism that increased expression of SMN protein, the correction of cellular pathologies including muscle physiology, and the benefits on survival were not reported (*33*). Because of the

NIH-PA Author Manuscript

NIH-PA Author Manuscript

NIH-PA Author Manuscript

similarities of the ASO sequence in the two studies, the improvements in efficacy in the current study are likely attributable to the MOE chemistry. Indeed, a side-by-side comparison of both chemistries in the CNS of a mouse model of mild SMA showed that the MOE chemistry provided more efficient modulation of splicing, improved in vivo stability, and decreased cellular inflammation compared to the 2′-OMe chemistry (*36*). The poor in vivo performance of 2′-OMe–based ASOs makes this chemistry less ideal for the clinic, as it would likely require a substantially greater number and frequency of administrations compared to the more active and better tolerated MOE chemistry. Furthermore, the in vivo efficacy of ASO-10-27 exceeded other more complex strategies that use nucleic acids to modulate *SMN2* splicing, such as transplicing and bi-functional RNAs (*37*–*39*).

The pharmacokinetic and pharmacodynamic data for ASO-10-27 showed that 8 μg/g was a pharmacologically active tissue concentration for increasing SMN protein levels in the spinal cord. Although there was a decrease in the ASO tissue concentration between 3 and 16 days, the amount of exon *7* inclusion and SMN protein peaked at 16 days. The inability to sustain elevated levels of SMN protein at 30 days suggests that the ASO tissue concentration at 16 days was not capable of modulating splicing; hence, the minimal concentration required for efficacy must be greater than 2 to 3 μg of ASO per gram tissue. The loss of SMN protein by 30 days is consistent with the Kaplan-Meier survival curve showing a median survival of 26 days. The pharmaco-dynamic profile in neonatal mice corroborated an earlier report in the adult SMA type III mouse model. Intracerebroventricular infusion of ASO-10-27 in adult SMA type III mice loaded the spinal cord with ASO (10 μg/g tissue), resulting in >90% of the *SMN2* transcripts containing exon *7* (*36*). However, the ASO tissue concentration of 10 μg/g in the type III SMA mouse model was sustained for at least 2 months, and the effect on splicing was maintained for at least 6 months (*36*). It is unclear why the pharmacokinetic data differ between the two models. It is possible that the developing and growing neonate may promote the cellular depletion of the ASO more rapidly than that in the adult. Regardless, it is reasonable to predict that the pharmaco-kinetic data in the current neonatal study might be a more relevant indicator of the kinetic profile to be encountered in infants and young children with SMA.

A necessary prerequisite for antisense product development is to demonstrate that the spinal cord of a large animal, such as a NHP, can achieve therapeutic concentrations of ASOs after a clinically viable route of delivery. There are multiple parameters predicted to influence the efficiency of ASOs to target the spinal cord parenchyma, including but not limited to the site of infusion, the dose and volume of the ASO to be infused, and the duration and rate of infusion. Our data showed that intrathecal infusion of a fixed dose of 3 mg was sufficient to load the spinal cord with therapeutic levels (>8 μg/g *tissue*) of ASO-10-27, and that increasing the infusion times of this fixed dose did not improve spinal cord loading. A 24-hour intrathecal infusion of 3 mg was well tolerated in monkeys and provided ASO (~20 μg/g) in the spinal cord. This demonstrates that a uniform RNA-based ASO can efficiently load the NHP spinal cord, which had been previously demonstrated only with intracerebroventricular infusions of an RNA-DNA hybrid ASO against superoxide dismutase–1 (*40*). Thus, intrathecal infusion is an effective delivery method for global distribution of splice-switching ASOs to the spinal cord of primates.

The eventual cause of death in ASO-10-27–treated SMA mice is not known. However, the sudden appearance of animals found dead, coupled with the observation of acute breathing abnormalities in end-stage SMA mice, suggests that cardiac and/or respiratory failure may be responsible. Cardiac failure (that is, bradycardia) thought to be caused by autonomic dysfunction was recently described in this severe mouse model and in SMA patients (*41*–*44*). In this scenario, a drop in the ASO tissue concentration in the lower brainstem may lead to the loss of autonomic function in the cardiac system, which would explain the sudden and

NIH-PA Author Manuscript

NIH-PA Author Manuscript

NIH-PA Author Manuscript

acute appearance of respiratory defects in ASO-10-27–treated SMA mice. A similar acute breathing aberration was observed in the long-lived scAAV8-hSMN–treated SMA mice (*12*). Analysis of the intercostal muscles of these mice showed that 85 to 90% of the neuromuscular junctions had a normal structure. Similarly, the current study showed that >95% of the intercostal neuromuscular junctions were normal in the ASO-10-27–treated SMA mice that lived beyond weaning age. These data suggest that the respiratory defects in the scAAV-hSMN– and ASO-10-27–treated SMA mice occurred independently of the skeletal muscles involved in breathing (*12*). However, additional studies are needed to confirm the role and relevance of the autonomic system in SMA disease.

In conclusion, delivery of ASO-10-27 to the CNS of mice with a severe form of SMA corrected the hallmark molecular, cellular, and functional phenotypes of this disease, and provided significant and reproducible survival benefits. The demonstration that a pharmacologically relevant tissue concentration—extrapolated from the mouse studies—could be attained throughout the NHP spinal cord indicates that intrathecal infusions may be an amenable route of delivery for ASO-10-27 in the clinic. We thus achieved our primary objectives of correcting SMA phenotypes in mice, identifying the tissue concentration required for efficacy, and verifying that this concentration can become loaded into the spinal cord using a clinically viable delivery strategy. Future studies in large-animal models that investigate the optimal metrics for delivery (for example, bolus versus slow infusion, catheter placement, and timing and frequency of repeat administration) and safety will be required to determine the feasibility of translating ASO-10-27 to the clinic.

MATERIALS AND METHODS

Oligonucleotides

The single-stranded MOE ASO-10-27 and MOE ASO-mismatch were generated as reported (*29, 45*). The sequence of ASO-10-27 was 5′-TCACTTTCATAATGCTGG-3′ and ASO-mismatch was 5′-TCATTTGCTTCATACAGG-3′ (the six mismatches are underlined). The lyophilized ASOs were suspended in saline to a final concentration of 10 μg/μl that was confirmed by ultraviolet (UV) spectrometry, sterilized through a 45-μm filter, and diluted with saline to the appropriate concentration for each injection dose.

Animal procedures

All protocols in mice and monkeys met ethical standards for animal experimentation and were approved by the Institutional Animal Care and Use Committees. Heterozygote ($Smn^{+/-}$, $hSMN2^{+/+}$, $SMN\Delta7^{+/+}$) breeding pairs were mated and genotyped as reported (*46*). On the day of birth, SMA ($Smn^{-/-}$, $hSMN2^{+/+}$, $SMN\Delta7^{+/+}$) pups were cryo-anesthetized and injected with 2 μl of ASO into each cerebral lateral ventricle for a total of 4 μl per pup. Injections were performed with a pulled capillary needle under the guidance of a transilluminator as reported (*47*). All the litters were culled so that each litter contained all the SMA pups plus two wild-type ($Smn^{+/+}$, $hSMN2^{+/+}$, $SMN\Delta7^{+/+}$) pups to control for litter size. The NHP experiment was performed at the Northern Biomedical Research (Muskegon, MI). Cynomolgus monkeys weighing 3 to 4 kg were anesthetized and implanted with intrathecal indwelling catheters. The monkeys were allowed to recover from the implantation surgery for several days before receiving intrathecal infusions via a programmable CADD-Micro 5900 pump (Smiths Medical). A total dose of 3 mg was infused over 1 day (3 mg/day), 3 days (1 mg/day), 7 days (0.43 mg/day), or 14 days (0.21 mg/day). Another cohort of monkeys underwent stereotactic surgery to implant a cannula into the right cerebral lateral ventricle as reported (*40*). These monkeys were infused with either 3 mg of ASO-10-27 (0.21 mg/day) or saline for 14 days.

NIH-PA Author Manuscript

NIH-PA Author Manuscript

NIH-PA Author Manuscript

Quantitative reverse transcription–polymerase chain reaction

Total RNA was extracted with Ambion MagMAX-96 RNA isolation kit (Applied Biosystems), reverse-transcribed, amplified with TaqMan One-Step RT-PCR Master Mix Kit (Applied Biosystems), and analyzed on an ABI PRISM 7500 Real-Time PCR System (Applied Biosystems). The expression levels for *SMN2* mRNA that contained exon *7* were normalized to glyceraldehyde-3-phosphate dehydrogenase (*GAPDH*) mRNA levels. The following primer probe sets were used to quantify exon *7* inclusion: forward primer, 5′-GCTGATGCTTTGGGAAGTATGTTA-3′; reverse primer, 5′-CACCTTCCTTCTTTTTGATTTTGTC-3′; probe, 5′-6-*FAM*-TACATGAGTGGCTATCATACT-*MGB*-3′ (GAPDH primer and probe set; Applied Biosystems).

ASO tissue concentration

The tissue concentration of ASO-10-27 in the mouse spinal cord was determined as reported (*48*). Briefly, the cervical, thoracic, and lumbar regions were homogenized and extracted with phenol-chloroform, analyzed by capillary gel electrophoresis, and quantified with standard curves of electropherogram peak area ratios or by the extinction coefficient method (*48*). For the NHP study, a hybridization-based enzyme-linked immunosorbent assay (ELISA) method was used to quantify oligonucleotide concentrations in tissue, because this procedure shows greater sensitivity and dynamic range compared to capillary gel electrophoresis (*49*).

Western blotting

The quantification of SMN protein levels was performed by Western blotting as reported (*12*). The nitrocellulose membrane was incubated with a mouse anti-SMN monoclonal antibody (1:5000 BD Biosciences), a rabbit anti–β-tubulin polyclonal antibody (1:750, Santa Cruz Bio-technology), and IRDye infrared secondary antibodies (1:20,000, LI-COR Biosciences).

Immunohistochemistry

Frozen tissue sections were incubated with a rabbit polyclonal antibody against the phosphorothioate backbone at 1:5000 dilution and visualized in the mouse or monkey with a donkey anti-rabbit secondary antibody conjugated to fluorescein isothiocyanate (FITC) (Jackson Laboratories) or with a 3,3′-diaminobenzidine (DAB) kit (Vector Laboratories), respectively. Motor neurons were labeled with an antibody against mouse ChAT as reported (*12*).

Motor neuron counting

Cells in the spinal cord ventral horn that exhibited a fluorescent ChAT signal were counted. About 8 to 10 different levels of each spinal cord region were analyzed to generate the average number of motor neurons per spinal cord region for each animal. Each section was at least 100 μm apart to prevent double counting of the same cell.

Myofiber size

Fixed quadriceps and intercostal muscles were processed by paraffin and stained for H&E to determine the myofiber cross-sectional size as reported (*17*). About 500 myofibers from each muscle were randomly selected, and the cross-sectional area of each myofiber was measured with MetaMorph (Molecular Devices) to calculate the average myofiber size per muscle for each animal.

NIH-PA Author Manuscript

NIH-PA Author Manuscript

NIH-PA Author Manuscript

Neuromuscular junction staining

In toto staining of fixed quadriceps and intercostal muscles was performed as reported (*12*). Presynaptic nerve terminals were labeled with a rabbit polyclonal antibody against neurofilament medium (Millipore), and acetylcholine receptors were labeled with Alexa 555–conjugated α-bungarotoxin (Molecular Probes). A minimum of 100 neuromuscular junctions from each muscle were randomly selected and assessed under the microscope to quantify the number of collapsed neuromuscular junctions for each muscle group per animal.

Behavioral tests

The righting reflex, grip strength, and hindlimb splay are validated tests for SMA mice (*50*). The righting reflex determined the time taken for the mouse to reposition itself onto all four paws after being placed in a supine position. In the grip strength, the forelimbs and hindlimbs were gently dragged horizontally along a wire mesh and the resistance was recorded (Columbia Instruments). In the hindlimb splay test, mice were suspended for 5 s by their tails and the resulting splay was determined by an arbitrary scoring system (*12*).

Statistics

The data used for statistical analysis were collected by blinded observers. The statistics in Figs. 2, 3E, 4E, and 5, A to F, were analyzed with one-way analysis of variance (ANOVA) and Bonferroni multiple post hoc comparisons. The Kaplan-Meier survival curve in Fig. 5G was analyzed with the log-rank test equivalent to the Mantel-Haenszel test. All statistical analyses were performed with GraphPad Prism v4.0 (GraphPad Software). Values with $P < 0.05$ were considered significant.

Supplementary Material

Refer to Web version on PubMed Central for supplementary material.

Acknowledgments

We thank T. Taksir, K. Misra, M. DeRiso, M. Phipps, D. Wagner, L. Curtin, and D. Matthews from Genzyme Corporation and B. Boyle and M. Butts from Northern Bio medical Research.

REFERENCES AND NOTES

1. Lefebvre S, Bürglen L, Reboullet S, Clermont O, Burlet P, Viollet L, Benichou B, Cruaud C, Millasseau P, Zeviani M, Le Paslier D, Frézal J, Cohen D, Weissenbach J, Munnich A, Melki J. Identification and characterization of a spinal muscular atrophy-determining gene. Cell. 1995; 80:155–165. [PubMed: 7813012]
2. Crawford TO, Pardo CA. The neurobiology of childhood spinal muscular atrophy. Neurobiol. Dis. 1996; 3:97–110. [PubMed: 9173917]
3. Sumner CJ. Therapeutics development for spinal muscular atrophy. NeuroRx. 2006; 3:235–245. [PubMed: 16554261]
4. McAndrew PE, Parsons DW, Simard LR, Rochette C, Ray PN, Mendell JR, Prior TW, Burghes AH. Identification of proximal spinal muscular atrophy carriers and patients by analysis of SMN^T and SMN^C gene copy number. Am. J. Hum. Genet. 1997; 60:1411–1422. [PubMed: 9199562]
5. Lorson CL, Hahnen E, Androphy EJ, Wirth B. A single nucleotide in the *SMN* gene regulates splicing and is responsible for spinal muscular atrophy. Proc. Natl. Acad. Sci. U.S.A. 1999; 96:6307–6311. [PubMed: 10339583]
6. Monani UR, Lorson CL, Parsons DW, Prior TW, Androphy EJ, Burghes AH, McPherson JD. A single nucleotide difference that alters splicing patterns distinguishes the SMA gene *SMN1* from the copy gene *SMN2*. Hum. Mol. Genet. 1999; 8:1177–1183. [PubMed: 10369862]

NIH-PA Author Manuscript

NIH-PA Author Manuscript

NIH-PA Author Manuscript

7. Cartegni L, Krainer AR. Disruption of an SF2/ASF-dependent exonic splicing enhancer in *SMN2* causes spinal muscular atrophy in the absence of *SMN1*. Nat. Genet. 2002; 30:377–384. [PubMed: 11925564]
8. Sumner CJ. Molecular mechanisms of spinal muscular atrophy. J. Child Neurol. 2007; 22:979–989. [PubMed: 17761653]
9. Prior TW, Swoboda KJ, Scott HD, Hejmanowski AQ. Homozygous *SMN1* deletions in unaffected family members and modification of the phenotype by *SMN2*. Am. J. Med. Genet. A. 2004; 130A: 307–310. [PubMed: 15378550]
10. Azzouz M, Le T, Ralph GS, Walmsley L, Monani UR, Lee DC, Wilkes F, Mitrophanous KA, Kingsman SM, Burghes AH, Mazarakis ND. Lentivector-mediated *SMN* replacement in a mouse model of spinal muscular atrophy. J. Clin. Invest. 2004; 114:1726–1731. [PubMed: 15599397]
11. Foust KD, Wang X, McGovern VL, Braun L, Bevan AK, Haidet AM, Le TT, Morales PR, Rich MM, Burghes AH, Kaspar BK. Rescue of the spinal muscular atrophy phenotype in a mouse model by early postnatal delivery of *SMN*. Nat. Biotechnol. 2010; 28:271–274. [PubMed: 20190738]
12. Passini MA, Bu J, Roskelley EM, Richards AM, Sardi SP, O'Riordan CR, Klinger KW, Shihabuddin LS, Cheng SH. CNS-targeted gene therapy improves survival and motor function in a mouse model of spinal muscular atrophy. J. Clin. Invest. 2010; 120:1253–1264. [PubMed: 20234094]
13. Valori CF, Ning K, Wyles M, Mead RJ, Grierson AJ, Shaw PJ, Azzouz M. Systemic delivery of scAAV9 expressing SMN prolongs survival in a model of spinal muscular atrophy. Sci. Transl. Med. 2010; 2:35ra42.
14. Corti S, Nizzardo M, Nardini M, Donadoni C, Salani S, Ronchi D, Saladino F, Bordoni A, Fortunato F, Del Bo R, Papadimitriou D, Locatelli F, Menozzi G, Strazzer S, Bresolin N, Comi GP. Neural stem cell transplantation can ameliorate the phenotype of a mouse model of spinal muscular atrophy. J. Clin. Invest. 2008; 118:3316–3330. [PubMed: 18769634]
15. Corti S, Nizzardo M, Nardini M, Donadoni C, Salani S, Ronchi D, Simone C, Falcone M, Papadimitriou D, Locatelli F, Mezzina N, Gianni F, Bresolin N, Comi CP. Embryonic stem cell-derived neural stem cells improve spinal muscular atrophy phenotype in mice. Brain. 2010; 133:465–481. [PubMed: 20032086]
16. Duque S, Joussemet B, Riviere C, Marais T, Dubreil L, Douar AM, Fyfe J, Moullier P, Colle MA, Barkats M. Intravenous administration of self-complementary AAV9 enables transgene delivery to adult motor neurons. Mol. Ther. 2009; 17:1187–1196. [PubMed: 19367261]
17. Avila AM, Burnett BG, Taye AA, Gabanella F, Knight MA, Hartenstein P, Cizman Z, Di Prospero NA, Pellizzoni L, Fischbeck KH, Sumner CJ. Trichostatin A increases SMN expression and survival in a mouse model of spinal muscular atrophy. J. Clin. Invest. 2007; 117:659–671. [PubMed: 17318264]
18. Narver HL, Kong L, Burnett BG, Choe DW, Bosch-Marcé M, Taye AA, Eckhaus MA, Sumner CJ. Sustained improvement of spinal muscular atrophy mice treated with trichostatin A plus nutrition. Ann. Neurol. 2008; 64:465–470. [PubMed: 18661558]
19. Butchbach ME, Singh J, Thorsteinsdóttir M, Saieva L, Slominski E, Thurmond J, Andrésson T, Zhang J, Edwards JD, Simard LR, Pellizzoni L, Jarecki J, Burghes AH, Gurney ME. Effects of 2,4-diaminoquinazoline derivatives on SMN expression and phenotype in a mouse model for spinal muscular atrophy. Hum. Mol. Genet. 2010; 19:454–467. [PubMed: 19897588]
20. Garbes L, Riessland M, Hölker I, Heller R, Hauke J, Tränkle C, Coras R, Blümcke I, Hahnen E, Wirth B. LBH589 induces up to 10-fold SMN protein levels by several independent mechanisms and is effective even in cells from SMA patients non-responsive to valproate. Hum. Mol. Genet. 2009; 18:3645–3658. [PubMed: 19584083]
21. Riessland M, Ackermann B, Förster A, Jakubik M, Hauke J, Garbes L, Fritzsche I, Mende Y, Blumcke I, Hahnen E, Wirth B. SAHA ameliorates the SMA phenotype in two mouse models for spinal muscular atrophy. Hum. Mol. Genet. 2010; 19:1492–1506. [PubMed: 20097677]
22. Mattis VB, Ebert AD, Fosso MY, Chang CW, Lorson CL. Delivery of a read-through inducing compound, TC007, lessens the severity of a spinal muscular atrophy animal model. Hum. Mol. Genet. 2009; 18:3906–3913. [PubMed: 19625298]

NIH-PA Author Manuscript

NIH-PA Author Manuscript

NIH-PA Author Manuscript

23. Tsai LK, Tsai MS, Ting CH, Li H. Multiple therapeutic effects of valproic acid in spinal muscular atrophy model mice. J. Mol. Med. 2008; 86:1243–1254. [PubMed: 18649067]
24. Hastings ML, Berniac J, Liu YH, Abato P, Jodelka FM, Barthel L, Kumar S, Dudley C, Nelson M, Larson K, Edmonds J, Bowser T, Draper M, Higgins P, Krainer AR. Tetracyclines that promote *SMN2* exon 7 splicing as therapeutics for spinal muscular atrophy. Sci. Transl. Med. 2009; 1:5ra12.
25. Mercuri E, Bertini E, Messina S, Solari A, D'Amico A, Angelozzi C, Battini R, Berardinelli A, Boffi P, Bruno C, Cini C, Colitto F, Kinali M, Minetti C, Mongini T, Morandi L, Neri G, Orcesi S, Pane M, Pelliccioni M, Pini A, Tiziano FD, Villanova M, Vita G, Brahe C. Randomized, double-blind, placebo-controlled trial of phenylbutyrate in spinal muscular atrophy. Neurology. 2007; 68:51–55. [PubMed: 17082463]
26. Swoboda KJ, Scott CB, Reyna SP, Prior TW, LaSalle B, Sorenson SL, Wood J, Acsadi G, Crawford TO, Kissel JT, Krosschell KJ, D'Anjou G, Bromberg MB, Schroth MK, Chan GM, Elsheikh B, Simard LR. Phase II open label study of valproic acid in spinal muscular atrophy. PloS One. 2009; 4:e5268. [PubMed: 19440247]
27. Oskoui M, Kaufmann P. Spinal muscular atrophy. Neurotherapeutics. 2008; 5:499–506. [PubMed: 19019300]
28. Hua Y, Vickers TA, Baker BF, Bennett CF, Krainer AR. Enhancement of *SMN2* exon 7 inclusion by antisense oligonucleotides targeting the exon. PLoS Biol. 2007; 5:e73. [PubMed: 17355180]
29. Hua Y, Vickers TA, Okunola HL, Bennett CF, Krainer AR. Antisense masking of an hnRNP A1/A2 intronic splicing silencer corrects *SMN2* splicing in transgenic mice. Am. J. Hum. Genet. 2008; 82:834–848. [PubMed: 18371932]
30. Singh NK, Singh NN, Androphy EJ, Singh RN. Splicing of a critical exon of human survival motor neuron is regulated by a unique silencer element located in the last intron. Mol. Cell. Biol. 2006; 26:1333–1346. [PubMed: 16449646]
31. Singh NN, Shishimorova M, Cao LC, Gangwani L, Singh RN. A short antisense oligonucleotide masking a unique intronic motif prevents skipping of a critical exon in spinal muscular atrophy. RNA Biol. 2009; 6:341–350. [PubMed: 19430205]
32. Singh NN, Singh RN, Androphy EJ. Modulating role of RNA structure in alternative splicing of a critical exon in the spinal muscular atrophy genes. Nucleic Acids Res. 2007; 35:371–389. [PubMed: 17170000]
33. Williams JH, Schray RC, Patterson CA, Ayitey SO, Tallent MK, Lutz GJ. Oligonucleotide-mediated survival of motor neuron protein expression in CNS improves phenotype in a mouse model of spinal muscular atrophy. J. Neurosci. 2009; 29:7633–7638. [PubMed: 19535574]
34. Bennett CF, Swayze EE. RNA targeting therapeutics: Molecular mechanisms of antisense oligonucleotides as a therapeutic platform. Annu. Rev. Pharmacol. Toxicol. 2010; 50:259–293. [PubMed: 20055705]
35. Rochette CF, Gilbert N, Simard LR. *SMN* gene duplication and the emergence of the *SMN2* gene occurred in distinct hominids: *SMN2* is unique to *Homo sapiens*. Hum. Genet. 2001; 108:255–266. [PubMed: 11354640]
36. Hua Y, Sahashi K, Hung G, Rigo F, Passini MA, Bennett CF, Krainer AR. Antisense correction of SMN2 splicing in the CNS rescues necrosis in a type III SMA mouse model. Genes Dev. 2010; 24:1634–1644. [PubMed: 20624852]
37. Baughan TD, Dickson A, Osman EY, Lorson CL. Delivery of bifunctional RNAs that target an intronic repressor and increase SMN levels in an animal model of spinal muscular atrophy. Hum. Mol. Genet. 2009; 18:1600–1611. [PubMed: 19228773]
38. Coady TH, Lorson CL. Trans-splicing-mediated improvement in a severe mouse model of spinal muscular atrophy. J. Neurosci. 2010; 30:126–130. [PubMed: 20053895]
39. Lorson CL, Rindt H, Shababi M. Spinal muscular atrophy: Mechanisms and therapeutic strategies. Hum. Mol. Genet. 2010; 19:R111–R118. [PubMed: 20392710]
40. Smith RA, Miller TM, Yamanaka K, Monia BP, Condon TP, Hung G, Lobsiger CS, Ward CM, McAlonis-Downes M, Wei H, Wancewicz EV, Bennett CF, Cleveland DW. Antisense oligonucleotide therapy for neurodegenerative disease. J. Clin. Invest. 2006; 116:2290–2296. [PubMed: 16878173]

NIH-PA Author Manuscript

NIH-PA Author Manuscript

NIH-PA Author Manuscript

41. Bevan AK, Hutchinson KR, Foust KD, Braun L, McGovern VL, Schmelzer L, Ward JG, Petruska JC, Lucchesi PA, Burghes AH, Kaspar BK. Early heart failure in the SMNΔ7 model of spinal muscular atrophy and correction by postnatal scAAV9-SMN delivery. Hum. Mol. Genet. 2010; 19:3895–3905. [PubMed: 20639395]

42. Bach JR. Medical considerations of long-term survival of Werdnig-Hoffmann disease. Am. J. Phys. Med. Rehabil. 2007; 86:349–355. [PubMed: 17449979]

43. Rudnik-Schöneborn S, Heller R, Berg C, Betzler C, Grimm T, Eggermann T, Eggermann K, Wirth R, Wirth B, Zerres K. Congenital heart disease is a feature of severe infantile spinal muscular atrophy. J. Med. Genet. 2008; 45:635–638. [PubMed: 18662980]

44. Hachiya Y, Arai H, Hayashi M, Kumada S, Furushima W, Ohtsuka E, Ito Y, Uchiyama A, Kurata K. Autonomic dysfunction in cases of spinal muscular atrophy type 1 with long survival. Brain Dev. 2005; 27:574–578. [PubMed: 15876504]

45. Baker BF, Lot SS, Condon TP, Cheng-Flournoy S, Lesnik EA, Sasmor HM, Bennett CF. 2′-*O*-(2-Methoxy)ethyl-modified anti-intercellular adhesion molecule 1 (ICAM-1) oligonucleotides selectively increase the ICAM-1 mRNA level and inhibit formation of the ICAM-1 translation initiation complex in human umbilical vein endothelial cells. J. Biol. Chem. 1997; 272:11994–12000. [PubMed: 9115264]

46. Le TT, Pham LT, Butchbach ME, Zhang HL, Monani UR, Coovert DD, Gavrilina TO, Xing L, Bassell GJ, Burghes AM. SMNΔ7, the major product of the centromeric survival motor neuron (*SMN2*) gene, extends survival in mice with spinal muscular atrophy and associates with full-length SMN. Hum. Mol. Genet. 2005; 14:845–857. [PubMed: 15703193]

47. Snyder EY, Taylor RM, Wolfe JH. Neural progenitor cell engraftment corrects lysosomal storage throughout the MPS VII mouse brain. Nature. 1995; 374:367–370. [PubMed: 7885477]

48. Leeds JM, Graham MJ, Truong L, Cummins LL. Quantitation of phosphorothioate oligonucleotides in human plasma. Anal. Biochem. 1996; 235:36–43. [PubMed: 8850544]

49. Yu RZ, Baker B, Chappell A, Geary RS, Cheung E, Levin AA. Development of an ultrasensitive noncompetitive hybridization–ligation enzyme-linked immunosorbent assay for the determination of phosphorothioate oligodeoxynucleotide in plasma. Anal. Biochem. 2002; 304:19–25. [PubMed: 11969184]

50. Butchbach ME, Edwards JD, Burghes AH. Abnormal motor phenotype in the SMNΔ7 mouse model of spinal muscular atrophy. Neurobiol. Dis. 2007; 27:207–219. [PubMed: 17561409]

NIH-PA Author Manuscript

NIH-PA Author Manuscript

NIH-PA Author Manuscript

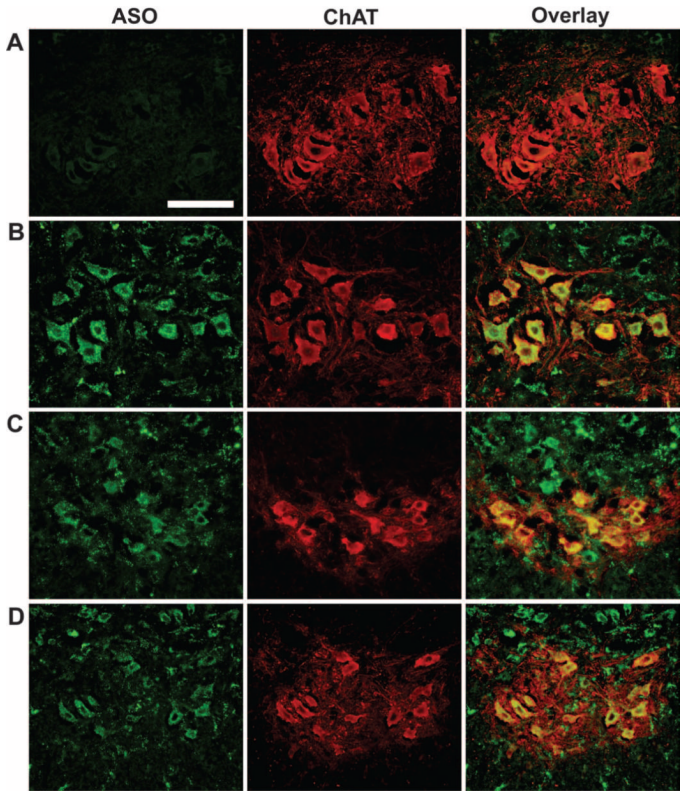

Fig. 1.

Targeting ASO-10-27 oligonucleotides to the mouse CNS. ASO-10-27 was efficiently targeted to motor neurons of the spinal cord of neonatal mice 14 days after intracerebroventricular injection. Double immunohistochemical staining was performed for the phosphorothioate backbone of the oligo-nucleotide (first column) and mouse choline acetyltransferase (ChAT; second column). (**A** to **D**) Colocalization signals (third column) are shown for the cervical (B), thoracic (C), and lumbar (D) regions of the spinal cord after ASO-10-27 treatment; control saline-treated mice did not show colocalization (A). Scale bar, 100 μm.

NIH-PA Author Manuscript
NIH-PA Author Manuscript
NIH-PA Author Manuscript

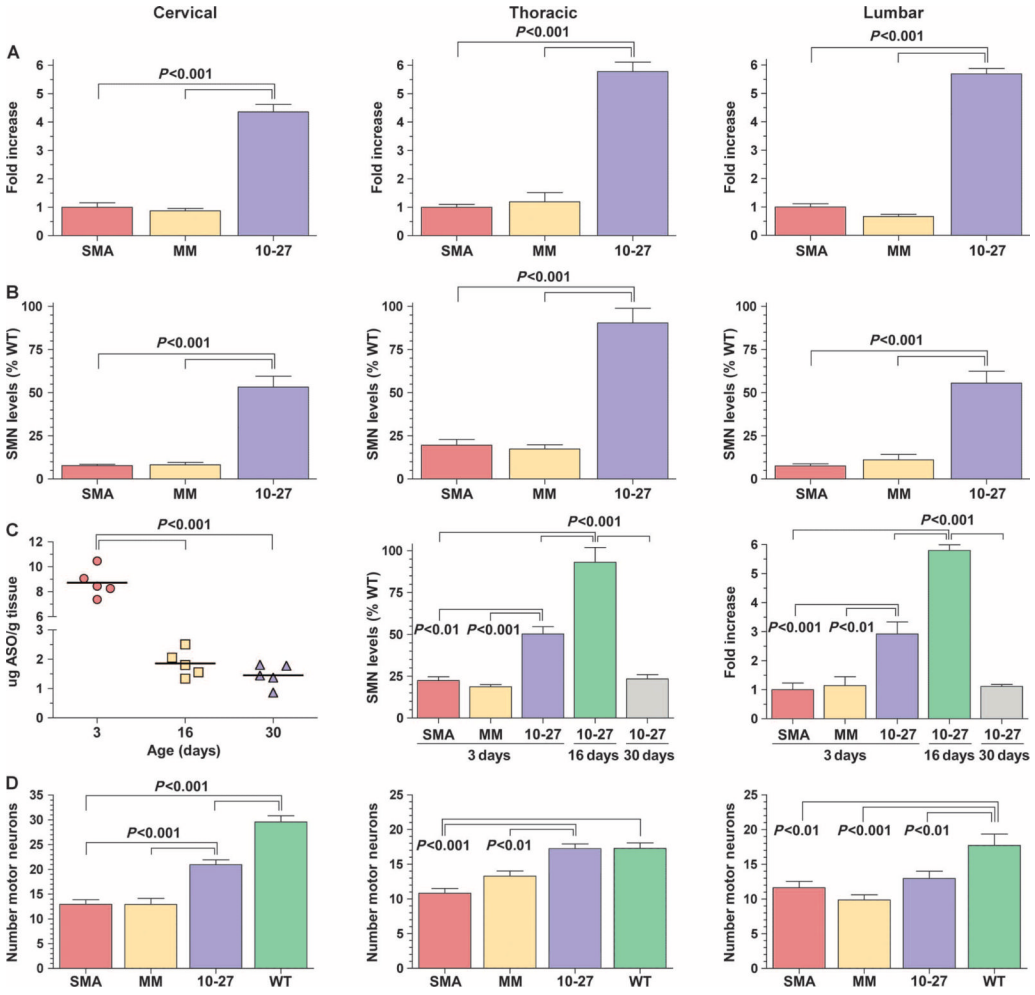

Fig. 2.

ASO-10-27 treatment boosts SMN protein expression in SMA mice. Treatment with ASO-10-27 increased exon *7* inclusion during *SMN2* splicing, and increased SMN protein expression and the numbers of motor neurons in the spinal cord after intracerebroventricular injection of neonatal mice with severe SMA at postnatal day 0 (P0). (**A**) The amount of *SMN2* mRNA that contained exon *7* relative to *SMN2* mRNA in untreated SMA mice was determined by reverse transcription–polymerase chain reaction (RT-PCR) at 16 days. (**B**) The amount of SMN protein relative to that in untreated wild-type (WT) mice was determined by Western blotting at 16 days. (**C**) For the pharmacodynamic/pharmacokinetic analysis, the absolute ASO tissue concentration in the cervical region was determined by capillary gel electrophoresis; the amount of SMN protein relative to that in untreated WT mice in the thoracic region was determined by Western blotting; and the amount of *SMN2* mRNA that contained exon *7* relative to that in untreated SMA mice in the lumbar region was determined by RT-PCR at 3, 16, and 30 days. (**D**) The number of motor neurons in the cervical, thoracic, and lumbar regions was determined by ChAT immuno-staining at 16 days. SMA, untreated SMA mice; MM, ASO-mismatch–treated SMA mice; 10-27, ASO-10-27–treated SMA mice; WT, untreated WT mice. The *P* values between the different treatment groups were determined by one-way ANOVA and Bonferroni multiple post hoc comparisons ($P < 0.01$; $P < 0.001$). Data are means ± SEM.

NIH-PA Author Manuscript

NIH-PA Author Manuscript

NIH-PA Author Manuscript

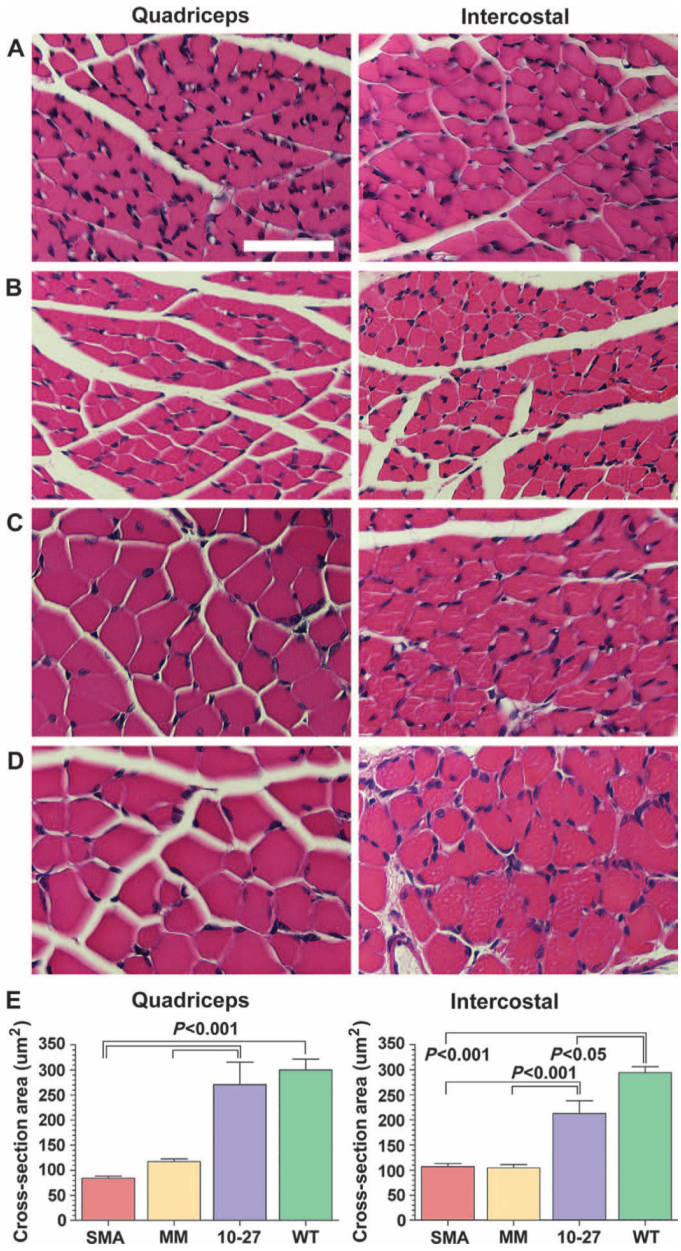

Fig. 3.

ASO-10-27 treatment increases myofiber size in SMA mice. (**A** to **D**) H&E staining of the quadriceps (left column) and intercostal (right column) muscles of untreated SMA mice (A), ASO-mismatch–treated SMA mice (B), ASO-10-27–treated SMA mice (C), and untreated WT mice (D) at 16 days. (**E**) The average myofiber cross-sectional area for each group was quantified. The *P* values between the different treatment groups were determined by one-way ANOVA and Bonferroni multiple post hoc comparisons ($P < 0.05$; $P < 0.001$). Data are means ± SEM. Scale bar, 50 μm.

NIH-PA Author Manuscript

NIH-PA Author Manuscript

NIH-PA Author Manuscript

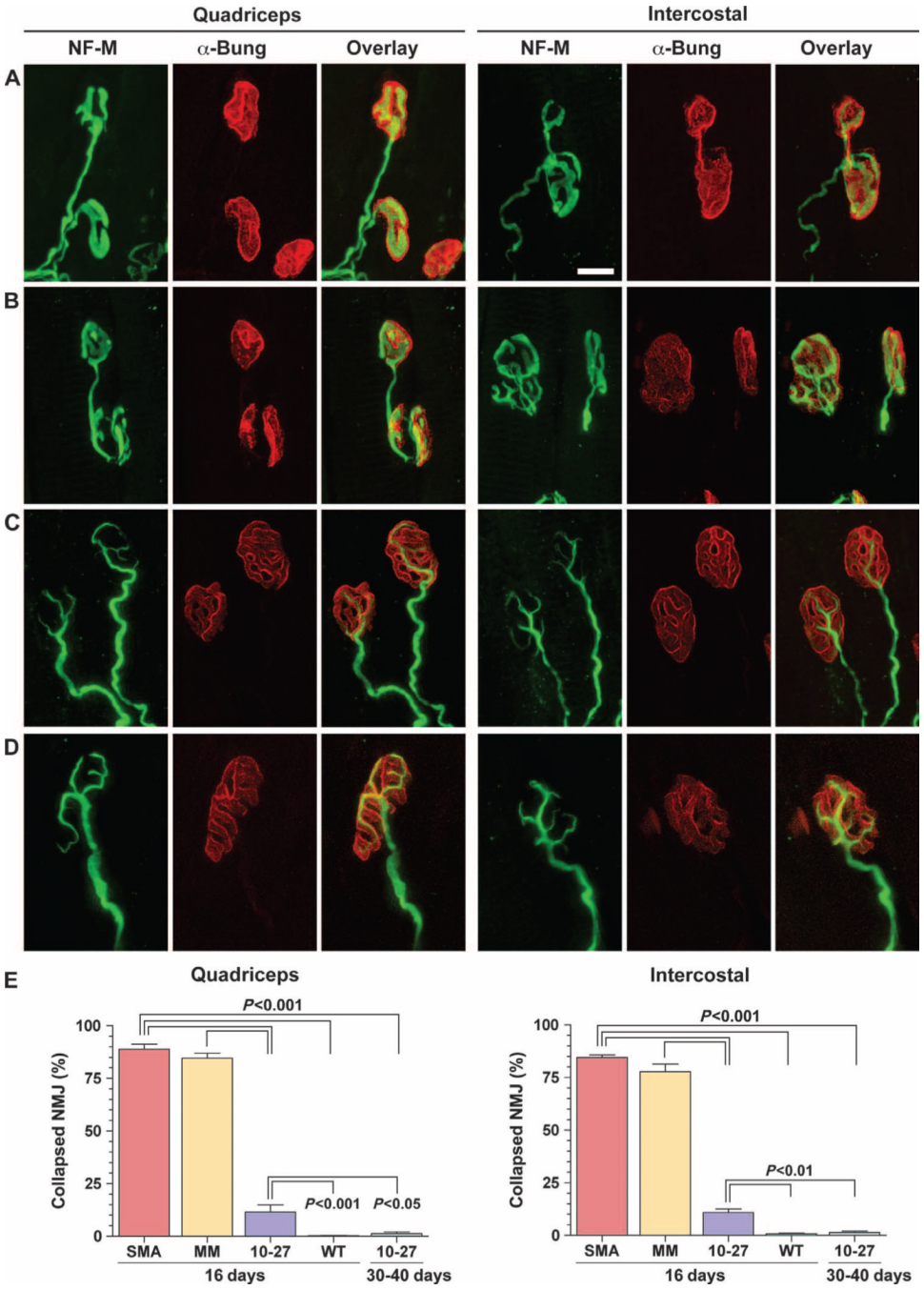

Fig. 4.

ASO-10-27 treatment improves neuromuscular junction structure in SMA mice. (**A** to **D**) In toto staining of muscle fibers from the quadriceps (*left column*) and intercostal (right column) muscles of untreated SMA mice (A), ASO-mismatch–treated SMA mice (B), ASO-10-27–treated SMA mice (C), and untreated WT mice (D) at 16 days. The axons of motor neurons at the presynaptic termini (green) were labeled with antibody to neurofilament medium (NF-M). The acetylcholine receptors of the postsynaptic termini were stained with α-bungarotoxin (α-Bung; red). The overlay of both signals (yellow) shows the innervation of the muscle and nerve at the motor end plate. As exemplified by the neuromuscular junctions in untreated SMA mice, the presynaptic termini displayed a

collapsed structure that typifies a pathological neuromuscular junction (A). (**E**) The percentage of neuromuscular junctions (NMJ) that contained this hallmark pathology was quantified at 16 and 30 to 40 days. The *P* values between the different treatment groups were determined by one-way ANOVA and Bonferroni multiple post hoc comparisons ($P < 0.05$; $P < 0.01$; $P < 0.001$). Data are means ± SEM. Scale bar, 10 μm.

NIH-PA Author Manuscript
NIH-PA Author Manuscript
NIH-PA Author Manuscript

NIH-PA Author Manuscript

NIH-PA Author Manuscript

NIH-PA Author Manuscript

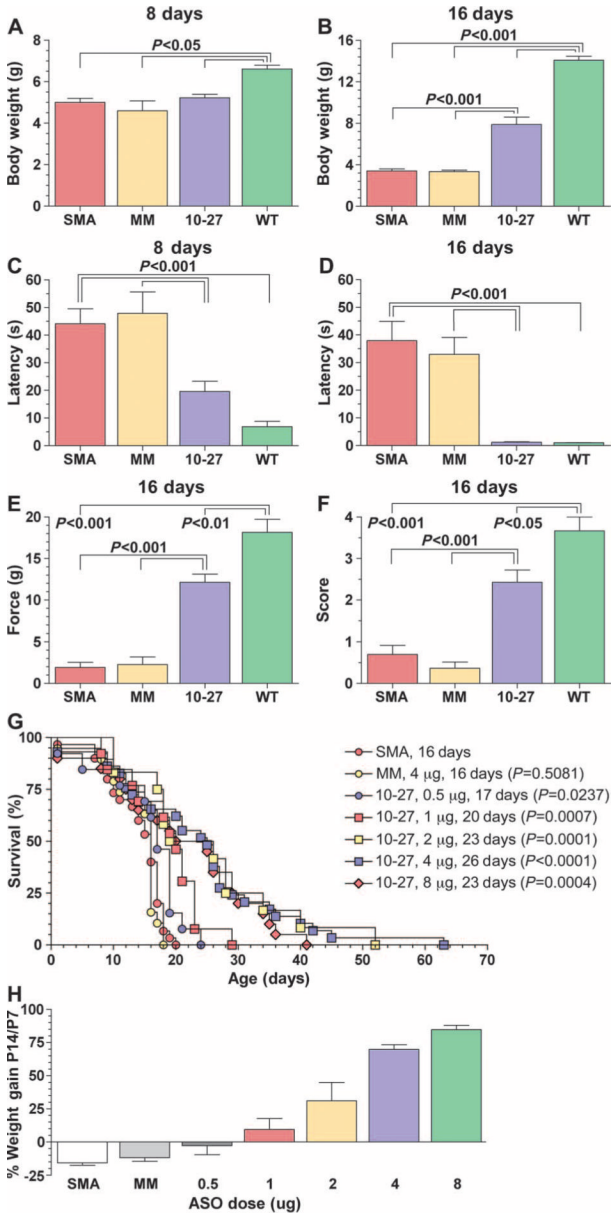

Fig. 5.

ASO-10-27 treatment improves function and survival of SMA mice. (**A** to **F**) Results of the body weight (A and B), righting reflex(C and D), gripstrength (E), and hindlimb splay (F) at 8 days (A and C) and 16 days (B, D, E, and F). (**G**) A single administration of different doses (0.5 to 8 μg) of ASO-10-27 was injected into P0 mice with severe SMA, and their survival was plotted on a Kaplan-Meier curve. The median survival was 18 to 26 days, which was a significant improvement compared to untreated SMA mice (0.5 μg, $P = 0.0237$; 1 μg, $P = 0.0007$; 2 μg, $P = 0.0001$; 4 μg, $P < 0.0001$; 8.0 μg, $P = 0.0004$). In contrast, SMA mice treated with ASO-mismatched oligonucleotides did not show an increase in survival (4 μg, $P = 0.5081$). (**H**) Percent weight gains between P14 and P7 with the different doses of ASO-10-27 in SMA mice. SMN, untreated SMA mice ($n = 18$); MM, SMA mice treated with 4 μg of ASO-mismatched oligonucleotide ($n = 14$); SMA mice treated with 0.5 μg ($n = 10$), 1 μg ($n = 9$), 2 μg ($n = 10$), 4 μg ($n = 20$), or 8 μg ($n = 13$) of ASO-10-27. The *P* values between the different treatment groups in (A) to (F) were determined by one-way ANOVA

and Bonferroni multiple post hoc comparisons ($P < 0.05$; $P < 0.01$; $P < 0.001$). The P values in the survival curve were analyzed with the Mantel-Haenszel test by comparing each treatment group to the untreated SMA group. Data are means ± SEM.

NIH-PA Author Manuscript
NIH-PA Author Manuscript
NIH-PA Author Manuscript

NIH-PA Author Manuscript

NIH-PA Author Manuscript

NIH-PA Author Manuscript

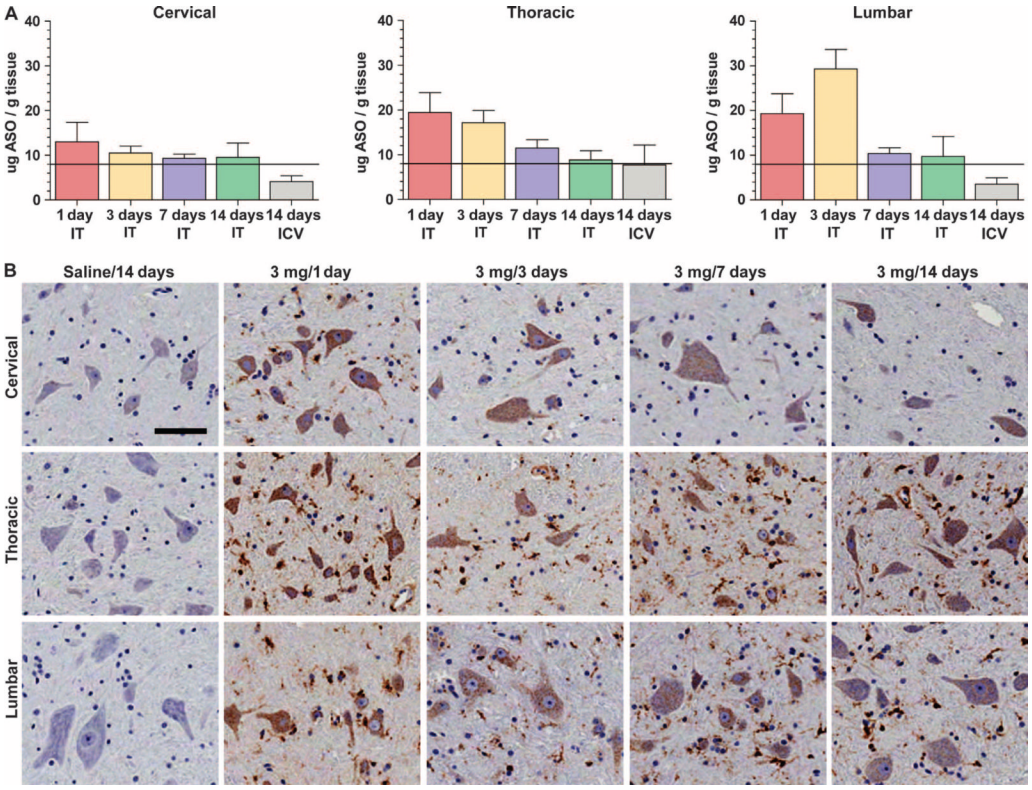

Fig. 6.

Therapeutic levels of ASO-10-27 in monkey spinal cord. Intrathecal (IT) and intracerebroventricular (ICV) infusions of ASO-10-27 loaded the monkey spinal cord with therapeutic levels (>8 μg/g) of the oligonucleotide. (**A**) ASO tissue concentrations in the cervical, thoracic, and lumbar regions after the administration of a 3-mg dose over different infusion times. (**B**) Immunohistochemical staining for the phosphorothioate backbone of ASO-10-27 showed a punctate intracellular signal in all ASO-10-27–treated groups, but not in monkeys that received saline. The immunopositive signal was detected in both large and small cell bodies, suggesting neuronal and glial uptake of the oligonucleotide. Data are means ± SEM. Scale bar, 100 μm.